

# Origin of catalytic activity differences between phosphine and phosphine oxide-based structures in the water-crosslinkable polyalkoxysilane composition

Shohei Tanaka<sup>1,2</sup> and Kenta Adachi<sup>\*1,3</sup>

<sup>1</sup>Department of Chemistry, Graduate School of Sciences and Technology for Innovation, Yamaguchi University, Yamaguchi, 753-8512, Japan

<sup>2</sup>Kuriyama R&D Inc., Sayama, Yamaguchi, 747-0849, Japan

<sup>3</sup>Opto-Energy Research Center, Yamaguchi University, Yamaguchi, 753-8511, Japan

Received: 20 November 2020, Accepted: 28 December 2020

## ABSTRACT

Organocatalysts have attracted enormous interest in the water-crosslinking reaction in silane-grafted polyolefins (SGPOs) system owing to their simplicity, low toxicity and environmentally benign nature compared to the organotin catalysts most commonly used in the SGPOs system. We focus on organophosphorus compounds including four structure types as organocatalysts; phosphoric acids, phosphoric esters, phosphine oxides and phosphine. Their catalytic activities for the water-crosslinking reaction in the 3-methacryloxypropyltrimethoxysilane grafted ethylene-propylene copolymer (EPR-g-MTMS) system were evaluated using the ATR-FTIR technique and the gel-fraction method. Phosphine oxides, phosphoric acids and phosphoric esters possessing an O=PR<sub>3</sub> or O=P(OR')<sub>3</sub> unit were found to be an excellent catalyst for the water-crosslinking reaction in the EPR-g-MTMS system, while phosphine (PR<sub>3</sub>) showed no catalytic activity on the water-crosslinking reaction in this system, indicating that the phosphoryl (P=O) unit plays an important role on the catalytic performance of these compounds. In comparison, phosphine oxides showed considerably higher catalytic activities than phosphoric acids/esters. Density functional theory (DFT) calculations demonstrated that the difference in catalytic activity could be attributed to an electron density at P=O unit making the activation for water through hydrogen-bonding. Finally, a possible catalytic mechanism for phosphoryl compounds in the EPR-g-MTMS system was proposed on the basis of these results and the S<sub>N</sub>2-Si pathway in silicate sol-gel chemistry. **Polyolefins J (2021) 8: 49-62**

**Keywords:** Phosphoryl compounds; water-crosslinking reaction; silane-grafting polyolefin; organocatalyst; hydrogen bonding.

## INTRODUCTION

Polyolefins (POs) are the largest-volume family of commercially important high-tonnage thermoplastic polymers. POs can be extruded into various types of products such as cables, pipes and films, while it is limited their services temperature to a lower level due to their low melt viscosity [1]. The conversion of the more or less linear structure of the POs into a three-dimensional structure was achieved by crosslinking. The

chemical crosslinking not only drastically improves a large number of properties such as thermomechanical properties, chemical and stress cracking resistance but also imparts to POs new useful properties such as shape memory. Ever since the development by Scott et al. in the 1970s [2], the water-crosslinkable silane-grafted polyolefins (SGPOs) have gained increasing attention from polymer industry due to the energy saving, low

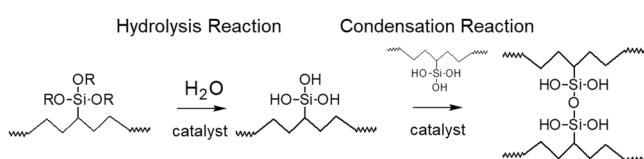
\*Corresponding Author - E-mail: k-adachi@yamaguchi-u.ac.jp

cost and high productivity [3-6]. Nowadays, SGPOs are used as key materials in the adhesive, sealant and coating technologies [7-8]. The water-crosslinking reaction occurs with hydrolysis and condensation reactions of alkoxy silane groups grafted on polyolefin backbones (Scheme 1) [9]. Even without any catalysts, the water-crosslinking reaction of SGPOs generally progresses in a slow manner. Therefore, catalysts for both hydrolysis and condensation reactions are necessary to promote the curing time and achieve the fully crosslinked materials. Organotin compounds (OTCs), such as a dibutyltin dilaurate or a dioctyltin dilaurate act as the catalysts to accelerate the water-crosslinking reaction in the SGPOs system [10-11]. However, OTCs are known to be toxic at relatively low levels of exposure, not only to marine invertebrates but also for mammals and other animals. Considering their strong toxic effects, the ban was already adopted in Europe and then finally by all the member countries of the United Nations Marine Environment Protection Committee. Therefore, there is a great need for a new eco-friendly catalytic system without OTCs in order to anticipate stronger limitations in the coming years.

In the field of silicate sol-gel science, the development of the organocatalysts for hydrolysis and condensation reactions of alkoxy silanes is one of the continuous motivations [12-13]. Several types of the organocatalysts, including Bronsted/Lewis acids or bases catalysts, have been utilized and proven to provide a beneficial metal-free sol-gel process for application in the biomedical and electronic fields. In particular, the organocatalytic sol-gel reaction of alkoxy silanes has been studied using organic acids such as carbonyl acids [14] and sulfonic acids [15], as well as organic bases such as amines [16], amidines [17], guanidines [18] and phosphazene [19]. Among them, it is well-known that  $P_4$ -t-Bu phosphazenes, which are the strong Lewis bases, play as the efficiency catalysts and promote the sol-gel reaction. The success of the

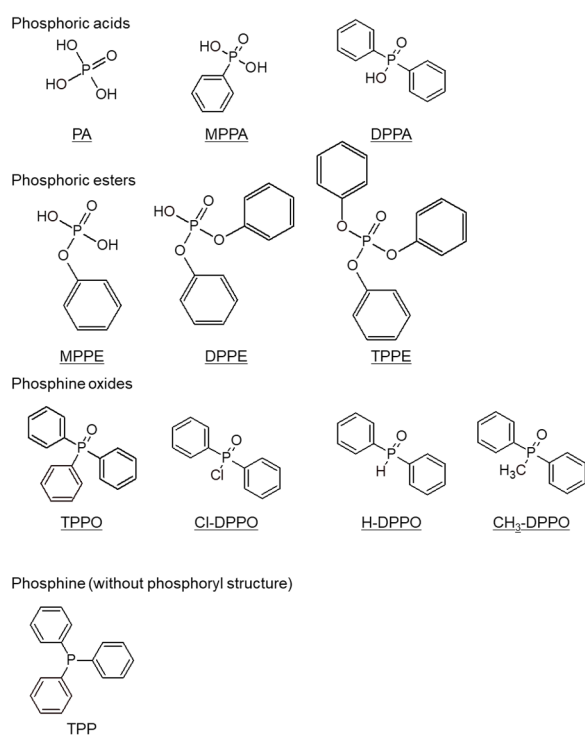
organocatalytic silicate sol-gel reaction has inspired us to apply them in the water-crosslinking reaction of SGPOs resins and develop a convenient method to control the crosslinking rate and density.

In this study, we focus on the organophosphorus compounds containing the phosphoryl ( $P=O$ ) functional group as candidates of new catalysts for the water-crosslinking reaction in SGPOs system. The organophosphorus compounds have been intensively investigated as the organocatalysts for several reactions [20-22] due to their highly dipolar and Lewis basicity [23-24]. Because Lewis basic  $P=O$  group plays as a proton-acceptor, it is well known that the phosphoryl compounds show the excellent catalytic performance for silylations of primary alcohols under the mild conditions [25-26]. Additionally, the organophosphorus compounds have many advantages over the above-mentioned organocatalysts for silicate sol-gel reaction. Note that the most significant point of the organophosphorus compounds is to enable to effectively catalyze the water-crosslinking reaction because of their low acidity, low toxicity, and sufficient chemical stability [27-28]. These properties are highly attractive for the industrial application to avoid the damage on the human and environment, which occurs in the case of using the strong acidic/basic catalysts. The goal of this study is to explore novel organocatalytic systems for the water-crosslinking reaction in SGPOs system using the organophosphorus compounds with various structures listed in Scheme 2. Herein, the catalytic performances of four different organophosphorus compounds (phosphonic acids, phosphoric esters and phosphine oxides, which are phosphoryl compounds general formula ( $O=P(OR')_3$  or  $O=PR_3$ ), and phosphine, which is organophosphorus compounds without  $P=O$  unit ( $PR_3$ )) on the water-crosslinking reaction in 3-methacryloxypropyltrimethoxysilane-grafted ethylene-propylene copolymer (EPR-g-MTMS) system were evaluated using ATR-FTIR technique and gel fraction measurement of crosslinked polymers. Kinetic investigations demonstrated that the phosphoryl compounds, in particular methyl(diphenyl)phosphine oxide, showed excellent catalytic activity for the water-crosslinking reaction in tested system. Additionally, density functional theory (DFT) calculations and molecular



**Scheme 1.** Water-crosslinking reaction pathway in silane-grafted polyolefin system.

### Phosphoryl (P=O) Compounds



**Scheme 2.** Organophosphorus compounds employed as organocatalysts for water-crosslinking reaction in EPR-g-MTMS system.

electrostatic potential (ESP) mappings were conducted in order to provide the mechanistic insight of the catalytic active site in the phosphoryl compounds. Interestingly, the Mulliken atomic charge at oxygen of P=O unit determined correlated well with the catalytic activities of the phosphoryl compounds. These results support the proposed conjugated Lewis base-catalytic mechanism of the phosphoryl compounds, whereby the P=O unit in a catalyst plays the dominant role to form the hydrogen-bonding and activate the water molecule in this system.

## EXPERIMENTAL

### Materials

The ethylene-propylene copolymer (EPR) used in this study was purchased from Clariant Japan. Some data of the EPR are presented in Table 1. Phosphoric acid (PA, Tokyo Chemical Industry (TCI) (Tokyo, Japan), >88%), phenylphosphonic acid (MPPA, TCI (Tokyo, Japan), >98%), diphenyl phosphinic acid (DPPA, TCI

(Tokyo, Japan), >98%), phenyl phosphate (MPPE, TCI (Tokyo, Japan), >99%), diphenyl phosphate (DPPE, TCI (Tokyo, Japan), >99%), triphenyl phosphate (TPPE, TCI (Tokyo, Japan), >99%), triphenylphosphine oxide (TPPO, TCI (Tokyo, Japan), >98%), methyl(diphenyl)phosphine oxide (CH<sub>3</sub>-DPPO, TCI (Tokyo, Japan), >98%), diphenylphosphinic chloride (Cl-DPPO, TCI (Tokyo, Japan), >98%), diphenylphosphine oxide (H-DPPO, TCI (Tokyo, Japan), >98%), triphenylphosphine (TPP, TCI (Tokyo, Japan), >95%), 3-methacryloxypropyltrimethoxysilane (MTMS, Aldrich (Penn., USA), 98%), dicumylperoxide (DCP, Aldrich (Penn., USA), 98%), xylene (Nacalai Tesque (Kyoto, Japan), >80%), acetone (Nacalai Tesque (Kyoto, Japan), >99%) and methanol (Nacalai Tesque (Kyoto, Japan), >99%) were used as received.

### Sample preparation

The grafting of MTMS onto EPR was performed following procedure [29]; The EPR granules were fed into a chamber at 120°C and allowed to melt for 15 min. After melting, the premixed MTMS/DCP was added. The chamber was then heated up to 180°C to proceed of grafting. The silane grafting yield was approximately 90% on the basis of MTMS. After grafting, the crosslink catalyst, in the amount of  $5.0 \times 10^{-4}$  mol/100g resin, was added. The 3-methacryloxypropyltrimethoxysilane-grafted ethylene-propylene copolymer (EPR-g-MTMS) with the organophosphorus compounds was removed from the chamber and shaped into approximately 1.0 mm thick compression-molded sheets by air pressing. To conduct a water-crosslinking reaction, the sample sheets were immersed into a water bath maintained at 30, 50 and 80°C for a defined time for examination of the reaction in progress. To avoid undesired water-crosslinking reaction while waiting for analysis of further treatment, the samples were kept under dried conditions.

**Table 1.** Ethylene-propylene copolymer characteristics used in this study.

| $M_w^{(a)}$<br>/kg mol <sup>-1</sup> | $M_r/M_w^{(a)}$ | Crystallinity <sup>(b)</sup><br>/wt. % | Ethylene<br>content <sup>(c)</sup> /mol % |
|--------------------------------------|-----------------|--|---|
| 27.7                                 | 0.43            | 34.9                                   | 10.1                                      |

<sup>(a)</sup> Number ( $M_n$ )- and weight ( $M_w$ )-averaged molecular masses

<sup>(b)</sup> Determined by wide-angle X-ray scattering

<sup>(c)</sup> Determined by <sup>13</sup>C NMR

## Analysis

Fourier transform infrared (FTIR) spectroscopy was used to follow the alkoxy silane hydrolysis and condensation reactions in EPR-g-MTMS system. The IR spectra were recorded using an AVATAR 370 (Thermo Nicolet (USA)) equipped with Smart Orbit Ge attenuated total reflectance accessory (Thermo Nicolet (USA)) in the range of 800-4000  $\text{cm}^{-1}$  with a resolution of 4  $\text{cm}^{-1}$ . The average of 32 spectra was used to increase the signal-to-noise ratio.

The gel contents of the crosslinked EPR-g-MTMS samples were determined by extracting the soluble fraction with boiling xylene for 6 h in a Soxhlet extractor [30]. The gel fraction was calculated as the percentage ratio of the dried weight of insoluble part ( $M_d$ ) to the initial weight ( $M_i$ ) as below equation;

$$\text{gel content (\%)} = \frac{M_d}{M_i} \times 100 \quad (1)$$

It is noted that prolonged extraction did not alter the gel content measurements for the selected samples, and EPR-g-MTMS samples that had not been water-crosslinked did not contain gel. According to the theory of Flory and Rehner [30], the average molecular weight between the crosslinks,  $M_c$ , is defined as follows;

$$M_c = -V\rho_p \frac{\left(\sqrt[3]{\phi_p} - \frac{\phi_p}{2}\right)}{\left[\ln(1 - \phi_p) + \phi_p + \chi\phi_p^2\right]} \quad (2)$$

where  $V$  is the molar volume of the solvent ( $V = 122 \text{ cm}^3/\text{mol}$ ),  $\rho_p$  is the polymer density ( $\rho_p = 0.89 \text{ g/cm}^3$ ),  $\phi_p$  is the volume fraction of polymer in the swollen gel, and  $\chi$  is the Flory-Huggins interaction parameter between solvent and polymer.  $M_c$  value is one of the most important structural parameters characterizing a crosslinked polymer, which is directly related to the crosslink density.  $\phi_p$  value is calculated as below:

$$\phi_p = \frac{\rho_s M_d}{\rho_s M_d + \rho_p M_s} \quad (3)$$

where  $\rho_s$  is the solvent density ( $\rho_s = 0.87 \text{ g/cm}^3$ ).  $M_s$  is the weight of the polymer swelled with solvent just after xylene extracting.

The Flory-Huggins interaction parameter between

solvent and polymer,  $\chi$ , is given by:

$$\chi = V \frac{(\delta_s - \delta_p)^2}{RT} \quad (4)$$

where  $\delta_s$  and  $\delta_p$  are the cohesive energy density of solvent and polymer, respectively. The  $\delta_s$  and  $\delta_p$  values used in this study are 18.3  $\text{MPa}^{0.5}$  and 15.2  $\text{MPa}^{0.5}$ , respectively [31].  $R$  and  $T$  indicate the universal gas constant and the absolute temperature (K), respectively.

## Quantum chemical calculations

All the theoretical calculations were performed using the Gaussian 09 programming package [32]. The geometrical optimizations of phosphoryl compounds applied as a catalyst in this study were calculated using the density functional theory (DFT) with a B3LYP functional, which was believed to be superior to the other two methods (ab-initio and MP2) in predicting molecular properties [33]. The 6-31 basis set was employed for C, H, P, and O atom containing molecules in all the calculations [34]. DFT calculation could yield to molecular structure and heat of formation. According to the procedure recommended by West et al. [35-36], the conformations of an intermediate for the hydrolysis and condensation were built by binding the oxygen atom of a nucleophilic complex to the silicon atom of an alkoxy silane and hydroxysilane, respectively, and then minimizing the energy with DFT calculation.

## RESULTS AND DISCUSSION

### Water-crosslinking reaction in silane-grafted polyolefin system in the presence of organophosphorus compounds

We found that the water-crosslinking reaction in 3-methacryloxypropyltrimethoxysilane-grafted ethylene-propylene copolymer (EPR-g-MTMS) system proceeded in the presence of phosphoryl compounds ( $\text{O}=\text{PR}_3$ ) acting as catalysts. The organophosphorus compounds evaluated in this study were classified based on their structure into the following four categories. Phosphoric acids [Phosphoric acid (PA), phenylphosphonic acid (MPPA) and diphenyl phosphinic acid (DPPA)], phosphoric esters [phenyl phos-

phate (MPPE), diphenyl phosphate (DPPE), triphenyl phosphate (TPPE)], phosphine oxides [triphenylphosphine oxide (TPPO), methyl(diphenyl)phosphine oxide ( $\text{CH}_3\text{-DPPO}$ ), diphenylphosphinic chloride ( $\text{Cl-DPPO}$ ), diphenylphosphine oxide ( $\text{H-DPPO}$ )] and phosphine [triphenylphosphine (TPP)]. The catalytic activities of organophosphorus compounds for the water-crosslinking reaction in this system were evaluated by two methods: attenuated total reflectance Fourier transform infrared spectroscopy (ATR-FTIR) measurement and gel fraction measurement. The former method is a powerful tool for monitoring the water-crosslinking reaction in this system and determining the reaction kinetics of the hydrolysis reaction ( $-\text{Si-OCH}_3 \rightarrow -\text{Si-OH}$ ). On the other hand, the later one is easily observable and evaluates the overall water-crosslinking reaction ( $-\text{Si-OCH}_3 \rightarrow -\text{Si-O-Si-}$ ).

Figure 1 shows the ATR-FTIR spectra collected for several aging times during the water-crosslinking reaction in EPR-g-MTMS system with TPPO as catalysts at  $80^\circ\text{C}$ . In the initial spectra, the absorption peaks at 1095 and  $1193\text{ cm}^{-1}$  correspond to Si-O stretching and Si-C stretching [37-38] of the methoxysilane groups ( $-\text{Si-OCH}_3$ ) in MTMS moieties, respectively; the intensities decrease monotonically with aging time. In the EPR-g-MTMS system with TPPO, the new absorption band at  $890\text{ cm}^{-1}$ , which is attributed to silanol ( $-\text{Si-OH}$ ), appears with aging time. With the further proceeding of water-crosslinking reaction, the new absorbance peaks at  $1048$  and  $1120\text{ cm}^{-1}$ , which correspond to single siloxane ( $-\text{Si-O-Si-}$ ) and multi-siloxane linkages ( $-\text{Si}=\text{O})_2\text{-Si-}$  or  $-\text{Si}\equiv\text{O})_3\text{-Si-}$ )

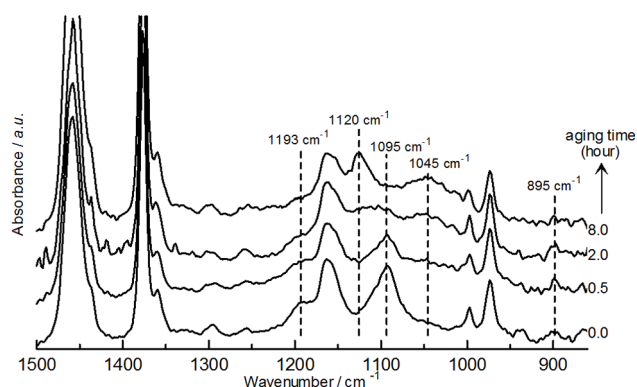


**Figure 1.** Spectral change due to the water-crosslinking reaction of EPR-g-MTMS in the presence of TPPO ( $5.0 \times 10^{-4}$  mol/100 g EPR resin) at  $80^\circ\text{C}$  measured by the ATR-FTIR technique. For peak assignment, see text.

[37-38], respectively, appear and increase, while the intensities at  $895\text{ cm}^{-1}$  gradually decrease with aging time. This result indicates that the successive condensation steps gradually occur after formation of hydrolyzed species in the EPR-g-MTMS system. Although minor differences did exist, similar spectral changes were observed in other systems. These results suggest that the degree of the water-crosslinking reaction in the EPR-g-MTMS system can be directly monitored using the ATR-FTIR technique.

In our previous study [29, 39-40], since the diffusion of water into the EPR-g-MTMS was not the rate-determining step of the water crosslinking reaction, the extent of the hydrolysis reaction of  $\text{Si-OCH}_3$  groups can be determined from the intensity ratio of the absorption peak at  $1095\text{ cm}^{-1}$  to the reference peak at  $1460\text{ cm}^{-1}$  ( $-\text{CH}_2-$  groups in EPR backbone). The dynamics of typical hydrolysis reaction conducted at various temperatures ( $30$ ,  $50$  and  $80^\circ\text{C}$ ) using PA, TPPE, TPPO and TPP, respectively, as catalysts are demonstrated in Figure 2, in which  $A_{1095}/A_{1460}$  ratios are plotted against aging time. Under these conditions, all tested systems were able to proceed the hydrolysis reaction of alkoxy silane groups in the EPR-g-MTMS system. For detail kinetic analysis of the hydrolysis reaction, the initial rate,  $r_{\text{hyd}}^0$  ( $\text{h}^{-1}$ ), of this reaction is defined as below:

$$r_{\text{hyd}}^0 = \left. \frac{d(A_{1095}/A_{1460})}{dt} \right|_{t=0} \quad (5)$$

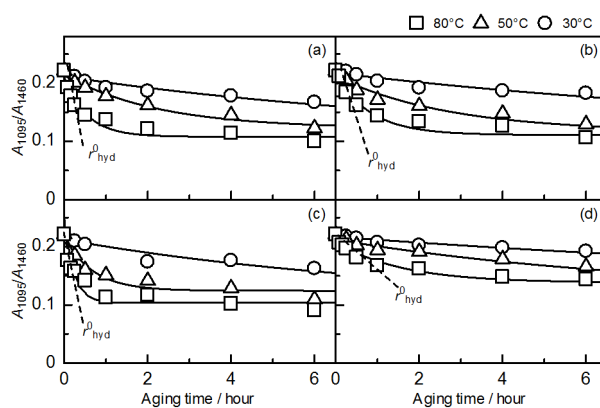


**Figure 2.** Time profile of  $A_{1095}/A_{1460}$  ratio of water-crosslinked EPR-g-MTMS in the presence of (a) PA, (b) TPPE, (c) TPPO, and (d) TPP at  $30$  (open circle),  $50$  (open triangle), and  $80^\circ\text{C}$  (open square).

The actual  $r_{\text{hyd}}^0$  values were assessed by differentiating the quadratic equation well-fitted to the observed points. The catalytic performance of TPP was poor, while the phosphoryl compounds such as TPPO, PA and TPPE significantly promoted the hydrolysis reaction in the EPR-*g*-MTMS system, indicating that the phosphoryl (P=O) unit in the catalyst was beneficial for enhancing their catalytic activities for hydrolysis reaction. Notably, the EPR-*g*-MTMS system containing TPPO exhibited the higher values of  $r_{\text{hyd}}^0$  than ones in the presence of other type catalysts. The activation energy is one of the indices for the evaluation of the catalytic activity. Generally, the catalyst with better catalytic activity has lower activation energy. The Arrhenius plot of the hydrolysis reaction in the EPR-*g*-MTMS with several catalysts is displayed in Figure 3. According to Arrhenius equation:

$$\ln r_{\text{hyd}}^0 = \ln A_{\text{hyd}} - \frac{E_{\text{a,hyd}}}{RT} \quad (6)$$

where  $A_{\text{hyd}}$  is the frequency factor,  $T$  is the absolute temperature,  $R$  is the gas constant and  $E_{\text{a,hyd}}$  is the activation energy for the hydrolysis reactions. The  $E_{\text{a,hyd}}$  values obtained from Figure 3 were listed in Table 2 to directly compare the catalytic activity of the organophosphorus compounds for the hydrolysis reaction in

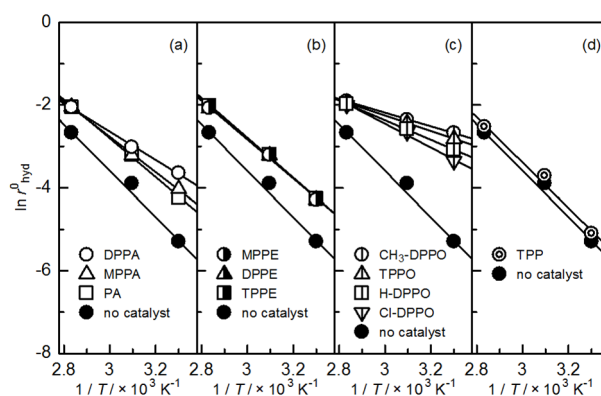


**Figure 3.** Plots of logarithmic hydrolysis rates as a function of reciprocal absolute temperature for EPR-*g*-MTMS in the presence of (a) phosphoric acids, (b) phosphoric esters, (c) phosphine oxides, and (d) phosphine. Solid lines were obtained from the analysis with Eq. (6).

this system. The value of  $E_{\text{a,hyd}}$  increased in the following order: phosphine oxides < phosphoric acids < phosphoric esters < phosphine  $\approx$  no catalysts. It can be inferred that the phosphine oxides show the best catalytic activity for the hydrolysis reaction in this system, as confirmed in Figure 2. Among the phosphine oxides,  $\text{CH}_3$ -DPPO showed significantly higher catalytic activity than other ones. Besides, in case of the phosphoric acids, it was found that  $E_{\text{a,hyd}}$  values remarkably depended on the number of hydroxyl group (-OH) in the structure. Interestingly, PA exhibited the

**Table 2.** Calculated Mulliken atomic charge on oxygen at phosphoryl (P=O) unit, activation energy of the hydrolysis ( $E_{\text{a,hyd}}$ ) and overall water-crosslinking reaction ( $E_{\text{a,crk}}$ ) for EPR-*g*-MTMS and the average molecular weight between cross-links ( $M_c$ ) for water-crosslinked EPR-*g*-MTMS.

|   | Catalyst <sup>(a)</sup> | Atomic charge <sup>(b)</sup> on oxygen at P=O group | Activation energy / kJ mol <sup>-1</sup> |                                   | Average molecular weight between crosslinks $M_c$ <sup>(e)</sup> /g mol <sup>-1</sup> |
|---|-------------------------|---|--|-----------------------------------|---|
|   |                         |   | $E_{\text{a,hyd}}$ <sup>(c)</sup>        | $E_{\text{a,crk}}$ <sup>(d)</sup> |   |
| <b>Phosphoric acids</b>                         | PA                      | -0.608  | 38.8 ± 0.5                               | 43.1 ± 1.2                        | (4.55 ± 0.09) × 10 <sup>4</sup>   |
|   | MPPA                    | -0.625  | 35.4 ± 1.5                               | 40.7 ± 1.0                        | (3.69 ± 0.08) × 10 <sup>4</sup>   |
|   | DPPA                    | -0.652  | 28.4 ± 0.2                               | 38.4 ± 0.5                        | (3.49 ± 0.15) × 10 <sup>4</sup>   |
| <b>Phosphoric esters</b>                        | MPPE                    | -0.598  | 39.2 ± 1.1                               | 44.7 ± 0.8                        | (4.58 ± 0.37) × 10 <sup>4</sup>   |
|   | DPPE                    | -0.602  | 38.3 ± 0.6                               | 43.6 ± 1.8                        | (4.62 ± 0.20) × 10 <sup>4</sup>   |
|   | TPPE                    | -0.602  | 39.9 ± 0.2                               | 43.8 ± 1.2                        | (4.65 ± 0.11) × 10 <sup>4</sup>   |
| <b>Phosphine oxides</b>                         | TPPO                    | -0.822  | 15.6 ± 0.8                               | 31.4 ± 0.8                        | (1.20 ± 0.08) × 10 <sup>4</sup>   |
|   | Cl-DPPO                 | -0.733  | 24.0 ± 0.2                               | 36.9 ± 0.3                        | (1.40 ± 0.10) × 10 <sup>4</sup>   |
|   | H-DPPO                  | -0.776  | 19.7 ± 0.2                               | 34.6 ± 0.6                        | (1.27 ± 0.05) × 10 <sup>4</sup>   |
|   | CH <sub>3</sub> -DPPO   | -0.900  | 13.7 ± 1.2                               | 30.4 ± 0.4                        | (1.11 ± 0.08) × 10 <sup>4</sup>   |
| <b>Phosphine without catalyst<sup>(f)</sup></b> | TPP                     | ---   | 45.5 ± 0.8                               | 64.0 ± 1.5                        | (10.09 ± 0.75) × 10 <sup>4</sup>  |
|   |                         | ---   | 46.5 ± 0.9                               | 66.4 ± 1.2                        |   |

<sup>(a)</sup>Catalyst concentration; 5.0 × 10<sup>-4</sup> mol/100 g EPR resin

<sup>(b)</sup>Obtained from DFT calculation at the B3LYP/6-31 level of theory.

<sup>(c)</sup>By means of ATR-FTIR

<sup>(d)</sup>By means of gel content

<sup>(e)</sup>Aged in 80 °C water for 24 h

<sup>(f)</sup>Ref. 29

maximum  $E_{a,hyd}$  value in the phosphoric acids catalysts ( $38.8 \text{ kJ mol}^{-1}$ ), which is almost equal to the value in the system containing phosphoric esters. Herein, it is noted that the catalytic activity of the phosphoric acids is not dependent on their acid dissociation constant,  $pK_a$  (PA: 1.83, MPPA: 1.83, DPPA: 2.32) [21]. These results indicate that the catalytic activities of the phosphoryl compounds are influenced by the difference in the substituent. In order to validate and understand the catalytic active site of the phosphoryl compounds tested in this study, density functional theory (DFT) calculations and molecular electrostatic potential (ESP) mappings were performed (results were not shown). ESP correlates with dipole moment, electronegativity, partial charges and the site of chemical reactivity of the molecule. It provides a visual method to understand the relative polarity of the molecule. Additionally, the atomic charges from Mulliken analysis were used to elucidate the nature of the P=O unit of the catalysts. The obtained values of Mulliken charge at oxygen atom of the P=O unit are also included in Table 2. As shown in Table 2, a significant downward of the Mulliken charge was observed with following: phosphine oxides < phosphoric acids < phosphoric esters. Clearly, there is a strong correlation between the  $E_{a,hyd}$  of the phosphoryl compounds and the Mulliken charge at oxygen atom at the P=O unit, i.e. the phosphine oxides with lower Mulliken charge result in higher catalytic activity correspondingly (Table 2). The ESP mapping demonstrated that the electron density was more localized on the P=O unit by decreasing the hydroxyl functional group in phosphoric acids. A possible explanation is that the high electron density on the P=O unit causes to enhance its Lewis basicity, making it preferential site in a nucleophilic attack [41-42]. Consequently, the kinetic and theoretical results indicate that the catalytic activities of the phosphoryl compounds for the hydrolysis reaction mainly depend on the Lewis basicity of the P=O unit. On the basis of these results, the catalytic mechanism of the phosphoryl compounds will be discussed below.

In general, the quantity of gel is used to evaluate the crosslinking degree of resins and rubbers [29]. In this study, the gel content measurement is used to study the kinetics of the overall water-crosslinking reaction in the EPR-g-MTMS system containing organophos-

phorous compounds. Figure 4 shows the time profile of gel contents of the crosslinked EPR-g-MTMS in the presence of PA, TPPE, TPPO and TPP. The degree of gel contents was found to be highly dependent on the catalyst and the aging temperature. Without the catalysts, the gel content was negligible after 6h. Conversely, in EPR-g-MTMS with TPPO system, the gel content has reached more than 85%. This was very favorable result compared to the EPR-g-MTMS system containing PA, TPPE and TPP. In the case of PA, TPPE and TPPO, the overall water-crosslinking reaction would be proceeded, however, 24 h were required to approach over 85% even at  $80^\circ\text{C}$ . To more precisely compare the catalytic activities for the overall water-crosslinking reaction, kinetic studies for each catalyst were performed. Initial overall water-crosslinking reaction rate,  $r_{crk}^0$  ( $\% \text{ h}^{-1}$ ), can be expressed using gel content value as below:

$$r_{crk}^0 = \left. \frac{d(\text{gel content})}{dt} \right|_{t=0} \quad (7)$$

The actual  $r_{crk}^0$  values were assessed by differentiating the quadratic equation well-fitted to the observed points. The effect of the catalysts on the initial overall water-crosslinking reaction is obvious; that is, EPR-g-MTMS with TPPO has a much faster initial overall water-crosslinking reaction rate than that with PA, TPPE and TPP. The difference in the initial rate can be ascribed to collisional efficiency, which is probably due to the diffusion behavior of the organophosphoryl compounds in the EPR-g-MTMS system. Although

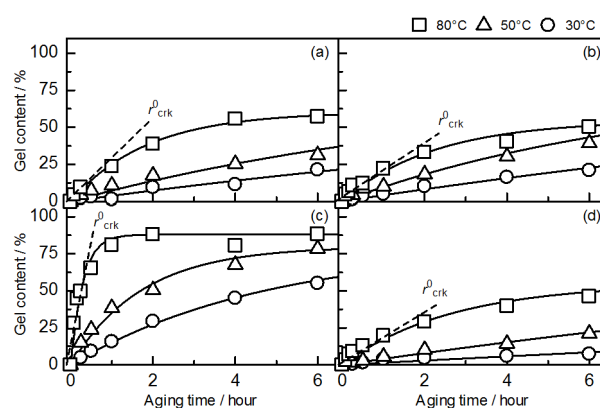


**Figure 4.** Time profile of gel content of water-crosslinked EPR-g-MTMS in the presence of (a) PA, (b) TPPE, (c) TPPO, and (d) TPP at 30 (open circle), 50 (open triangle), and  $80^\circ\text{C}$  (open square).

we cannot still measure the diffusion of organophosphoryl compounds in the EPR-g-MTMS system, these results clearly indicate that the initial overall water-crosslinking rate is affected by the catalysts structures. This finding may be very important in understanding a comprehensive catalytic mechanism for the water-crosslinking reaction, and will also be discussed in the next section. Figure 5 shows the plots of logarithmic initial overall water-crosslinking reaction rates of EPR-g-MTMS with various catalysts as a function of the reciprocal absolute temperature. These data can be well fitted with a straight line over a significant temperature range. According to Eq. (8), the activation energies for the overall water-crosslinking reaction were determined from the slope observed in the plots.

$$\ln r_{\text{crk}}^0 = \ln A_{\text{crk}} - \frac{E_{\text{a,crk}}}{RT} \quad (8)$$

where  $A_{\text{crk}}$  is the frequency factor for overall water-crosslinking reactions and  $E_{\text{a,crk}}$  is the activation energy for the overall water-crosslinking reactions. The least squares linear regression is very reliable ( $R^2 > 0.98$ ). The observed values of  $E_{\text{a,crk}}$  are also listed in Table 2. From Table 2, it is evident at a glance that the phosphoryl compounds, especially the phosphine oxides, also have a strong catalytic performance not only on the hydrolysis reaction but also on the overall water-crosslinking reaction of EPR-g-MTMS. As with the case of the hydrolysis reaction, the values of  $E_{\text{a,crk}}$  increased following order: phosphine oxides <

phosphoric acids < phosphoric esters < phosphine  $\approx$  no catalysts. This result indicates that the phosphine oxides possessing an  $\text{O}=\text{PR}_3$  have a high catalytic performance on the overall water-crosslinking reaction compared to phosphoric acids/esters ( $\text{O}=\text{P}(\text{OR}')_3$ ) and phosphine ( $\text{PR}_3$ ).

The molecular weight of the chains between cross-linked EPR,  $M_c$ , is an important parameter that determines how far a network can extend to accommodate solvent and solute molecules, and thus is a crucial property of the crosslinked network for the potential application of silane-grafted polyolefin resins [43]. This parameter was calculated using the Flory-Rehner equation as described above and the results are shown in Table 2. Their values remarkably depend on the catalysts type, indicated that the phosphoryl compounds also play an important role on the silane water-crosslinking network structure of the crosslinked EPR. The  $M_c$  values obtained by the phosphine oxides are considerably smaller than the ones obtained by the other catalysts, indicating the crosslinked EPR-g-MTMS catalyzed by phosphine oxides consisted of the high-density network structure. Based on the silicate sol-gel chemistry knowledge, under the base-catalyzed conditions, the sol-gel derived siloxane networks yield more highly branched clusters which do not interpenetrate prior to gelation and thus behave as discrete clusters (so-called “monomer-cluster growth”) [44-45]. Inspired by this knowledge, we concluded that the phosphoryl compounds-catalytic mechanism for the water-crosslinking reaction closely resembled the silicate hydrolysis-condensation reactions catalyzed by basic catalyst. The detail catalytic mechanism of the phosphoryl compounds will be discussed in the following section.

### Calculated equilibrium geometries for complexes with phosphine oxides and water molecule

The equilibrium geometries for complexes of  $\text{CH}_3$ -DPPO, TPPO, H-DPPO and Cl-DPPO with water molecule in vacuum were obtained at the B3LYP/6-31 level of theory, see Figure 6. In all case, there is a reasonably short POH hydrogen bond (1.78 – 1.86 Å). Moreover,  $\text{CH}_3$ -DPPO enabled to form the shorter hydrogen bond with water molecule than the other phosphine oxides. Experimentally, it was indeed observed

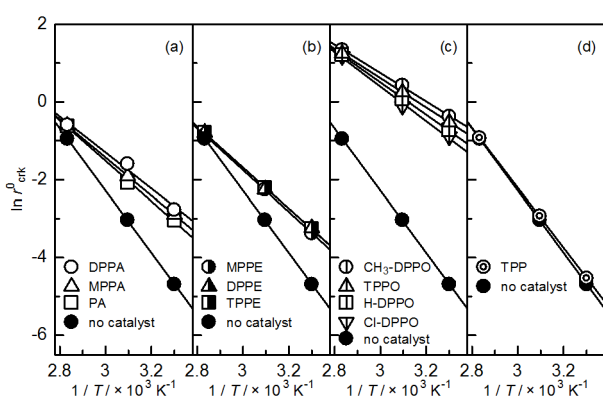


**Figure 5.** Plots of logarithmic overall water-crosslinking rates as a function of reciprocal absolute temperature for EPR-g-MTMS in the presence of (a) phosphoric acids, (b) phosphoric esters, (c) phosphine oxides, and (d) phosphine. Solid lines were obtained from the analysis with Eq. (8).

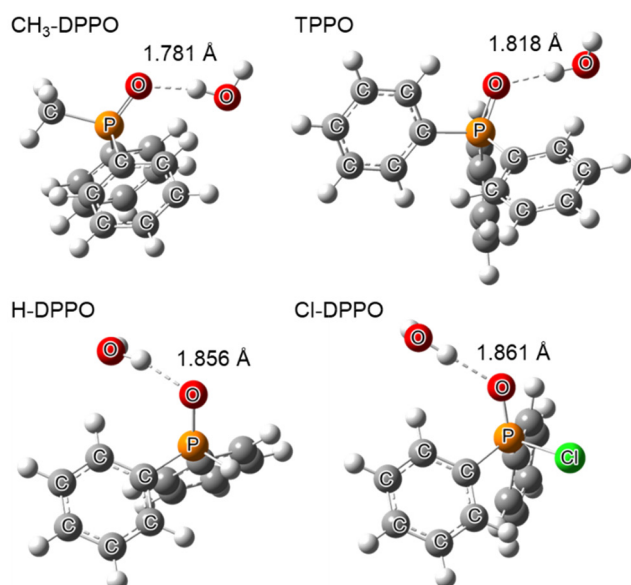


**Figure 6.** Calculated equilibrium structures of the complex of phosphine oxides with water molecule in vacuum. The bond length is given next to corresponding POH hydrogen bond.

that  $\text{CH}_3\text{-DPPO}$  was a stronger Lewis base than the others and the Lewis basicity of phosphine oxides was correlated to the hydrogen bond length obtained from the DFT calculation.

Additionally, a comprehensive computational study was conducted using the DFT theory to determine possible mechanistic pathways of the silane water-crosslinking reaction in the presence of phosphine oxides. To make the computational study tractable, methyltrimethoxysilane ( $\text{CH}_3\text{Si}(\text{OCH}_3)_3$ ) and trihydroxymethylsilane ( $\text{CH}_3\text{Si}(\text{OH})_3$ ) were selected for the model reaction. The reaction pathways were determined for the hydrolysis and the condensation reactions to form a silanol and siloxane, respectively, for the presence of phosphine oxides (TPPO,  $\text{CH}_3\text{-DPPO}$ , H-DPPO and Cl-DPPO). The heat of formation was calculated on the basis of total energy value for reactants, intermediates and products in the hydrolysis and

the condensation reactions, respectively. All energies of both reactions in the presence of phosphine oxides are listed in Table 3. The values of energy barrier were calculated for the hydrolysis and the condensation reaction in the presence of phosphine oxides according to Eq. (9):

$$\Delta H = H_{\text{inter}} - H_{\text{ini}} \quad (9)$$

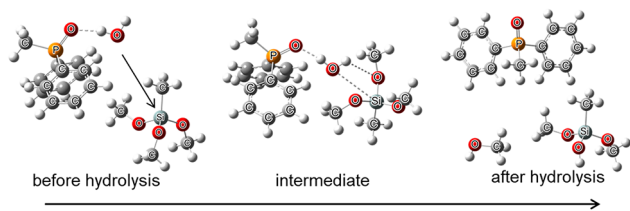
where  $H_{\text{ini}}$  and  $H_{\text{inter}}$  are the energies of reactants and intermediates in both reactions, respectively. As a configuration of typical results calculated by DFT, the hydrolysis reaction for  $\text{CH}_3\text{Si}(\text{OCH}_3)_3$  in the presence of  $\text{CH}_3\text{-DPPO}$  is shown in Figure 7. In an intermediate ( $\text{CH}_3\text{Si}(\text{OCH}_3)_3\text{-H}_2\text{O-CH}_3\text{-DPPO}$  complex) for the hydrolysis, its stability seems to arise from a penta-coordinated silicon and  $\text{O}\cdots\text{Si}$  and  $\text{O}\cdots\text{H}$  hydrogen bonds. Figure 8 shows the condensation reaction of two  $\text{CH}_3\text{Si}(\text{OH})_3$  in the presence of  $\text{CH}_3\text{-DPPO}$ . An intermediate consisted of  $\text{CH}_3\text{Si}(\text{OH})_3\text{-CH}_3\text{-DPPO}$  complex via a silanol-phosphoryl hydrogen bond, and another  $\text{CH}_3\text{Si}(\text{OH})_3$  was attained for condensation. The geometry most likely for condensation is similar to that for hydrolysis shown in Figure 7. Moreover, the energy barrier order for hydrolysis and condensation was of the same tendency ( $\text{CH}_3\text{-DPPO} < \text{TPPO} < \text{H-DPPO} < \text{Cl-DPPO}$ ). Although these results cannot directly deal with the reactions in the EPR-g-MTMS system, the results show a complex involvement between the phosphine oxide and the water molecule in suggesting the catalytic mechanism of phosphoryl compounds for the water-crosslinking reaction.

**Mechanism of water-crosslinking reaction in the EPR-g-MTMS system with phosphoryl compounds**  
On the basis of the phenomena described above, we have proposed a potential conjugated Lewis base cata-

**Table 3.** Heat of formation energies for reacts ( $H_{\text{ini}}$ ), intermediates ( $H_{\text{inter}}$ ) and products ( $H_{\text{prod}}$ ) in the hydrolysis and condensation reaction in the presence of several phosphine oxides ( $\text{CH}_3\text{-DPPO}$ , TPPO, H-DPPO and Cl-DPPO) and calculated energy gaps ( $\Delta H$ ).

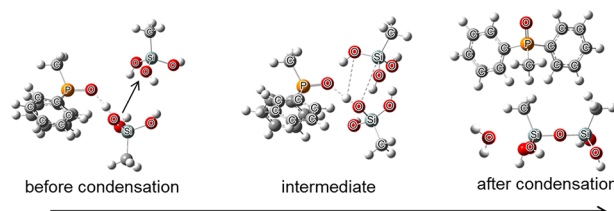
| Phosphine oxides<br>Catalyst | Hydrolysis              |                          |            |                         | Condensation            |                          |            |                         |
|------------------------------|-------------------------|--------------------------|------------|-------------------------|-------------------------|--------------------------|------------|-------------------------|
|                              | $H_{\text{ini}}^{(a)}$  | $H_{\text{inter}}^{(a)}$ | $\Delta H$ | $H_{\text{prod}}^{(a)}$ | $H_{\text{ini}}^{(a)}$  | $H_{\text{inter}}^{(a)}$ | $\Delta H$ | $H_{\text{prod}}^{(a)}$ |
|                              | / $10^7$ kJ mol $^{-1}$ |                          |            |                         | / $10^7$ kJ mol $^{-1}$ |                          |            |                         |
| <b>CH<sub>3</sub>-DPPO</b>   | -4370.77                | -4344.28                 | 26.48      | -4357.28                | -5336.81                | -5289.66                 | 47.15      | -5304.84                |
| <b>TPPO</b>                  | -4871.53                | -4844.31                 | 27.22      | -4857.32                | -5839.45                | -5787.04                 | 52.41      | -5805.04                |
| <b>H-DPPO</b>                | -4272.75                | -4242.32                 | 30.44      | -4257.37                | -5250.58                | -5187.70                 | 64.98      | -5204.94                |
| <b>Cl-DPPO</b>               | -5474.26                | -5441.50                 | 32.76      | -5459.67                | -6455.02                | -6386.85                 | 68.17      | -6407.24                |

<sup>(a)</sup>In vacuo calculated with B3LYP/6-31 at 298.15 K.



Hydrolysis Reaction

**Figure 7.** Geometries for  $\text{CH}_3$ -DPPO catalyzed hydrolysis reaction.

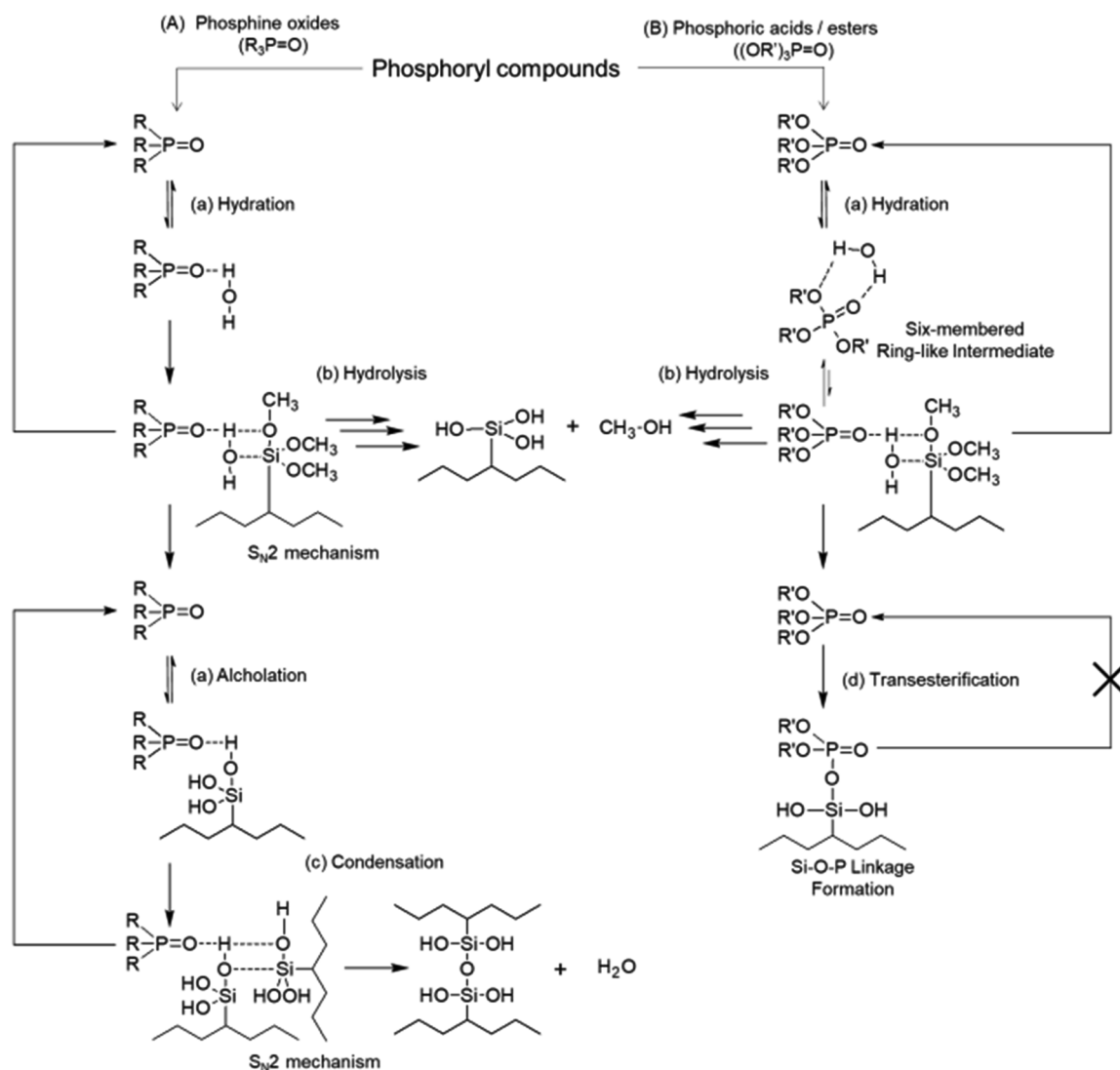


Condensation Reaction

**Figure 8.** Geometries for  $\text{CH}_3$ -DPPO catalyzed condensation reaction.

lytic mechanism of the phosphoryl compounds for the water-crosslinking reaction in the EPR-*g*-MTMS system. Scheme 3 shows the possible elementary pathways in the water-crosslinking reaction of EPR-*g*-MTMS using the phosphoryl compounds as catalysts. A water-crosslinking reaction is considered to be pro-

ceeded through the following steps: (a) hydrogen and oxygen atoms within the water molecules have polar covalent bonds. It is well-known that the chemical features of phosphoric acid and related compounds manifest themselves in the greater nucleophilicity of the phosphoryl oxygen and electrophilicity of the phos-



**Scheme 3.** Possible catalytic cycle for water-crosslinking reaction in silane-grafted polyolefin system with phosphoryl compounds.

phorus atom. Therefore, the phosphine oxide based compounds would readily form conjugated Lewis bases with water molecules (Scheme 3A). These conjugated Lewis bases act as strong nucleophilic species. (b) The nucleophilic water moiety of conjugated Lewis base naturally attacks the less-crowded back-side of silicon atom in an  $S_N2$  manner and then forms the ternary intermediate state (methoxysilane group/water/phosphoryl compound) via weak  $O\cdots Si$  and  $O\cdots H$  bonds, eventually leading to silanol, methanol, and original phosphoryl compounds. (c) Activation of the silanol group by the hydrogen-bonding complex of the phosphoryl catalyst similarly leads to an increase in the rate of siloxane bond (Si-O-Si) formation in the condensation step. At this stage, we do not have experimental evidence to support this path to form a nucleophilic attack on the silicon center of the alkoxysilane group. Nevertheless, a similar mechanism is widely adopted in kinetics to nucleophilic substitutions at the center of silicon in traditional silicate sol-gel chemistry. For example, Bassindale suggested that the conjugation of the silanol group and base catalyst via hydrogen-bonding leads to partial proton transfer from silanol group to the catalysts, resulting in the formation of the Si-O-Si linkages from the reaction between the conjugated Lewis base and another silanol group [46].

As shown in Figure 6 and Scheme 3, the conjugated Lewis base of the phosphoryl compound and the water molecule is a key structure to understand the origin of the catalytic efficiency of the phosphoryl compounds in the EPR-g-MTMS system. Note that phosphoric acids and phosphoric esters exhibited lower catalytic activities for both hydrolysis and overall water-crosslinking reactions than phosphine oxides. According to literature reported by Tolstoy et al. [47], phosphoric acids or phosphoric esters easily form the water-bridged cyclic dimers and trimers via the inter/intramolecular contiguous hydrogen bonds in the aqueous system. Consequently, opportunities for the  $S_N2$ -Si pathway via a nucleophilic attack may be restricted by the steric and electronic requirements of the comparatively bulky conjugated Lewis base in the EPR-g-MTMS system (Scheme 3B). It is well-known that phosphoric acid/esters show the high nucleophilic property of  $O=P(OR')_3$  unit, leading to the formation

of a network consisting of silicophosphate (Si-O-P) linkages by the transesterification reaction [48-50]. Phosphoric acids/esters are consumed to form Si-O-P linkages and eventually do not act as catalysts on the condensation steps. Further mechanistic studies are underway on the water-crosslinking reaction catalyzed by various phosphoryl compounds (conjugated Lewis bases).

## CONCLUSIONS

In conclusion, we have developed an organocatalytic water-crosslinking reaction in the 3-methacryloxy-propyltrimethoxysilane-grafted ethylene-propylene copolymer (EPR-g-MTMS) system using the various organophosphorus compounds as catalysts. Phosphoryl compounds, in particular phosphine oxides, were found to promote the water-crosslinking reaction more efficiently. Kinetic studies and DFT calculations indicated that the catalytic activity of the phosphoryl compounds depended on their Lewis basicity. Although the details of the catalytic mechanism are unknown, DFT calculations were performed to determine the relation with phosphine oxides and hydrogen donors, suggesting the formation of the hydrogen bonding leads to the nucleophilic activation of the water molecule in the reaction system. The use of phosphoryl compounds as catalysts will enable to expand the scope of the metal-free water-crosslinking reaction in the silane-grafted polyolefin system and may lead to the development of new advanced materials for industry and environment.

## ACKNOWLEDGEMENT

This study was partly supported by the Grant-in-Aid for Scientific Research (C) (Grant No. 19K05525) from Japan Society for the Promotion of Science (JSPS), the Adaptable and Seamless Technology transfer Program through Target-driven R&D (A-STEP) (Grant No. JPMJTM20GC) from Japan Science and Technology (JST), and the program of the Chugoku Regional Innovation Research Center, "The New Industrial Innovation Research Workshop". The authors thank the Core Clusters for Research Initia-

tives of Yamaguchi University, “Novel Analytical and Measuring Technology Contributions to Elucidation of Materials aiming at Life-Science Applications”.

## REFERENCES

- Boaen NK, Hillmyer MA (2005) Post-polymerization functionalization of polyolefins. *Chem Soc Rev* 34: 267-275
- Scott HG (1972 Feb 29) Crosslinking of a Polyolefin with a Silane, U.S. Patent 3, 646, 155
- Sirisinha K, Chimdist S (2008) Silane-crosslinked ethylene–octene copolymer blends: Thermal aging and crystallization study. *J Appl Polym Sci* 109: 2522-2528
- Sirisinha K, Boonkongkaew M, Kositchaiyong S (2010) The effect of silane carriers on silane grafting of high-density polyethylene and properties of crosslinked products. *Polym Test* 29: 958-965
- Han C, Bian J, Liu H, Han L, Wang S, Dong L, Chen S (2010) An investigation of the effect of silane water-crosslinking on the properties of poly(L-lactide). *Polym Inter* 59: 695-703
- Qiao J, Guo M, Wang L, Liu D, Zhang X, Yu L, Song W, Liu Y (2011) Recent advances in polyolefin technology. *Polym Chem* 2: 1611-1623
- Hanifpour A, Bahri-Laleh N, Nekoomanesh-Haghighi M (2020) Preparation of novel, liquid, solvent-free polyolefin-based adhesives. *Polym Adv Technol* 31: 922-931
- Hanifpour A, Bahri-Laleh N, Nekoomanesh-Haghighi M (2020) Methacrylate-functionalized POSS as an efficient adhesion promoter in olefin-based adhesives. *Polym Eng Sci* 60: 2991-3000
- Adachi K, Hirano T (2009) The utility of sulfonic acid catalysts for silane water-crosslinked network formation in the ethylene–propylene copolymer system. *J Sol-Gel Sci Technol* 49: 186-195
- Wang D, Klein J, Mejia E (2017) Catalytic systems for the cross-linking of organosilicon polymers. *Chem Asian J* 12: 1180-1197
- Cervantes J, Zarraga R, Salazar-Hernandez C (2012) Organotin catalysts in organosilicon chemistry. *Appl Organometal Chem* 26: 157-163
- Cypryk M, Gostyruski B, Pokora M, (2019) Hydrolysis of trialkoxysilanes catalysed by the fluoride anion. Nucleophilic vs. basic catalysis. *New J Chem* 43: 15222-15232
- Valliant EM, Jones JR (2011) Softening bioactive glass for bone regeneration: sol–gel hybrid materials. *Soft Matter* 7: 5083-5095
- Brinker CJ, Scherer GW (1990) Sol–gel science the physics and chemistry of sol–gel processing. Academic Press Inc., New York
- Sardon H, Engler AC, Chan JMW, Garcia JM, Coady DJ, Pascual A, Mecerreyes D, Jones GO, Rice JE, Horn HW, Hedrick JL (2013) Organic acid-catalyzed polyurethane formation via a dual-activated mechanism: Unexpected preference of N-activation over O-activation of isocyanates. *J Am Chem Soc* 135: 16235-16241
- Ignatyev IS, Montejo M, Gonzalez JLL (2009) Role of structures with penta- and hexacoordinate silicon in the nucleophile-catalyzed hydrolysis of tetramethoxysilane. *Phys Chem Chem Phys* 11: 841-847
- Bassindale AR, Liu Z, Mackinnon IA, Taylor PG, Yang Y, Light ME, Horton PN, Hursthouse MB (2003) A higher yielding route for T8 silsesquioxane cages and X-ray crystal structures of some novel spherosilicates. *Dalton Trans* 14: 2945-2949
- Fuchise K, Igarashi M, Sato K, Shimada S (2018) Organocatalytic controlled/living ring-opening polymerization of cyclotrisiloxanes initiated by water with strong organic base catalysts. *Chem Sci* 9: 2879-2891
- Kobayashi K, Ueno M, Kondo Y (2006) Phosphazene base-catalyzed condensation of trimethylsilylacetate with carbonyl compounds. *Chem Commun* 3128-3130
- Saito T, Aizawa Y, Tajima K, Isono T, Satoh T (2015) Organophosphate-catalyzed bulk ring-opening polymerization as an environmentally benign route leading to block copolyesters, end-functionalized polyesters, and polyester-based polyurethane. *Polym Chem* 6: 4374-4384
- Delgove MAF, Wroblewska AA, Stouten J, van Slagmaat CAMR, Noordijk J, De Wildeman SMA, Bernaerts KV (2020) Organocatalyzed ring opening polymerization of regio-isomeric

- lactones: Reactivity and thermodynamics considerations. *Polym Chem* 11: 3573-3584
22. Chen S, Wang H, Li Z, Wei F, Zhu H, Xu S, Xu J, Liu J, Gebru H, Guo K (2018) Metallic organophosphate catalyzed bulk ring-opening polymerization. *Polym Chem* 9: 732-742
  23. Gal JF, Maria PC, Yanez M, Mo O (2019) On the lewis basicity of phosphoramides: A critical examination of their donor number through comparison of enthalpies of adduct formation with  $SbCl_5$  and  $BF_3$ . *Chem Phys Chem* 20: 2566-2576
  24. Tupikina EY, Bondensteiner M, Tolstoy PM, Denisov GS, Shenderovich LG (2018)  $P=O$  moiety as an ambidextrous hydrogen bond acceptor. *J Phys Chem C* 122: 1711-1720
  25. Liu X, Verkada JG (2001) Electron-rich  $O = PR_3$  compounds: Catalysts for alcohol silylation. *Heteroat Chem* 12: 21-26
  26. Huang T, Saga Y, Guo H, Yoshimura A, Ogawa A, Han LB (2018) Radical hydrophosphorylation of alkynes with  $R_2P(O)H$  generating alkenylphosphine oxides: Scope and limitations. *J Org Chem* 83: 8743-8749
  27. Makiguchi K, Satoh T, Kakuchi T (2011) Diphenyl phosphate as an efficient cationic organocatalyst for controlled/living ring-opening polymerization of  $\delta$ -valerolactone and  $\epsilon$ -caprolactone. *Macromolecules* 44: 1999-2005
  28. Krasovec F, Jan J (1963) Investigation on the extraction of metal ions with different organophosphorus compounds. I. The dissociation, distribution and dimerization of some di-aryl esters of orthophosphoric acid. *Croat Chem Acta* 35: 183-193
  29. Tanaka S, Adachi K (2019) A novel efficient catalyst for water-crosslinking reaction of silane-grafted polyolefin system: Specific influence of axially coordinated n-alkylamine ligand on catalytic abilities of metal acetylacetonate complex. *Mater Today Commun* 21: 100584
  30. Bartob AFM (1983) *Handbook of Solubility Parameters and Other Cohesion Parameters*. Boca Raton
  31. Barton AFM (1985) *Applications of solubility parameters and other cohesion parameters in polymer science and technology*. *Pure Appl Chem* 57: 905-912
  32. Frisch M J, Trucks G, Schlegel H, Scuseria G, Cheeseman J, Scalmani G, Barone V, Mennucci B, Petersson G (2009) Gaussian 09 Revision D. 01. Gaussian, Inc., Wallingford CT
  33. Lee C, Yang W, Parr RG (1987) Development of the Colle-Salvetti correlation-energy formula into a functional of the electron density. *Phys Rev B* 37: 785-789
  34. Mclean AD, Chandler CS (1980) Contracted Gaussian basis sets for molecular calculations. I. Second row atoms,  $Z=11-18$ . *J Chem Phys* 72: 5639-5648
  35. West JK (1997) Theoretical analysis of hydrolysis of polydimethylsiloxane (PDMS). *J Biomed Mater Res* 35: 505-511
  36. West JK, Hench LL (1994) Silica fracture Part I. A ring contraction mode. *J Mater Sci* 29: 3601-3606
  37. Shieh YT, Liu CM (1999) Silane grafting reactions of LDPE, HDPE, and LLDPE. *J Appl Polym Sci* 74: 3404-3411
  38. Zhao Q, Liu Q, Xu H, Bei Y, Feng S (2016) Preparation and characterization of room temperature vulcanized silicone rubber using  $\alpha$ -amine ketoximesilanes as auto-catalyzed cross-linkers. *RSC Adv* 6: 38447-38453
  39. Adachi K, Hirano T (2008) Good linear relationship between logarithms of Eigen's water exchange constants for several divalent metal ions and activation energies of corresponding metal-catalyzed alkoxy silane hydrolysis in ethylene-propylene copolymer system. *Eur Polym J* 44: 542-549
  40. Adachi K, Hirano T (2008) Controllable silane water-cross-linking kinetics and curability of ethylene-propylene copolymer by amine compounds. *Ind Eng Chem Res* 47: 1812-1819
  41. Tan YC, Zeng HC (2018) Lewis basicity generated by localised charge imbalance in noble metal nanoparticle-embedded defective metal-organic frameworks. *Nature Com* 9: 4326
  42. Giba IS, Mulloyarova VV, Denisov GS, Tolstoy PM (2019) Influence of hydrogen bonds in 1:1 complexes of phosphinic acids with substituted pyridines on  $^1H$  and  $^{31}P$  NMR chemical shifts. *J Phys Chem A* 123: 2252-2260
  43. Tanaka F, Edwards SF (1992) Viscoelastic prop-

- erties of physically crosslinked networks. 1. Transient network theory. *Macromolecules* 25: 1516-1523
44. Aelion R, Loebel A, Eirich F (1950) Hydrolysis of ethyl silicate. *J Am Chem Soc* 72: 5705-5712
45. Grubb WT (1954) A rate study of the silanol condensation reaction at 25° in alcoholic solvents. *J Am Chem Soc* 76: 3408-3414
46. Bassindale AR, Chen H, Liu Z, Mackinnon A, Parker DJ, Taylor PG, Yang Y, Light ME, Horton PN, Hursthouse MB (2004) A higher yielding route to octasilsesquioxane cages using tetrabutylammonium fluoride, Part 2: Further synthetic advances, mechanistic investigations and X-ray crystal structure studies into the factors that determine cage geometry in the solid state. *J Organomet Chem* 689: 3287-3300
47. Mulloyarova VV, Giba IS, Denisov GS, Ostras AS, Tolstoy PM (2019) Conformational mobility and proton transfer in hydrogen-bonded dimers and trimers of phosphinic and phosphoric acids. *J Phys Chem A* 123: 6761-6771
48. Styskalik A, Babiak M, Machac P, Relichova B, Pinkas J (2017) New adamantane-like silicophosphate cage and its reactivity toward tris(pentafluorophenyl)borane. *Inorg Chem* 56: 10699-10705
49. Styskalik A, Skoda D, Moravec Z, Babiak M, Barenes CE, Pinkas J (2015) Control of micro/mesoporosity in non-hydrolytic hybrid silicophosphate xerogels. *J Mater Chem A* 3: 7477-7487
50. Weinberger C, Heckel T, Schnippering P, Schmitz M, Guo A, Keil W, Marsmann HC, Schmidt C, Tiemann M, Wilhelm R (2019) Straightforward immobilization of phosphonic acids and phosphoric acid esters on mesoporous silica and their application in an asymmetric aldol reaction. *Nanomaterials* 9: 249